



Preprint of work presented at the annual INMM meeting in Orlando Florida, July 18-22, 2004

Portable Video/Gamma Camera for Surveillance, Safeguards, Treaty Verification and Area Monitoring

James F. Christian, Michael R. Squillante, Mitchell Woodring, and Gerald Entine

Radiation Monitoring Devices, Inc.
Watertown, Massachusetts 02472, USA (617) 926-1167

Radiation Monitoring Devices, Inc.
44 Hunt Street
Watertown, MA 02472
(617) 926-1167 www.RMDInc.com

Portable Video/Gamma Camera for Surveillance, Safeguards, Treaty Verification and Area Monitoring

James F. Christian, Michael R. Squillante, Mitchell Woodring, and Gerald Entine
Radiation Monitoring Devices, Inc.
Watertown, Massachusetts 02472, USA (617) 926-1167

ABSTRACT

Detecting, identifying, monitoring, and tracking radioactive material and mapping its distribution has become a high-priority task. This paper reports the development of a self-contained, portable gamma camera combined with a video camera for locating, identifying and quantifying nuclear radiation sources. The system provides a two-dimensional image of the areas and the radiation source. It presents images of gamma radiation superimposed over a black and white video image of the same field of view. In addition, spectra showing the isotopes present are displayed for user-selected areas of the image. Multiple sources of differing energy can be located and identified. To facilitate the location and identification of nuclear materials, we have developed a data-manipulation scheme which allows a multi-dimensional data array, comprised of the x- and y-position coordinates, and the event energy, to be used in the imaging process. In the imager software, a gate can be set on a specific isotope energy to reveal where in the field of view the gated data lies or, conversely, a gate can be set on an area in the field of view to examine what isotopes are present in that area. By moving the instrument around a target a 3-dimension image can be formed giving the user the capability of locating sources inside buildings. The system operates over the energy range of 30 keV to 1.5 MeV with a detection limit better than 4×10^4 Bq for ^{137}Cs with similar sensitivity to Pu and U. Dynamic range is 10^4 Bq to over 10^{11} Bq. The operating system is Microsoft Windows.

I. INTRODUCTION

Detecting, monitoring, identifying and tracking radioactive material, for health physics, safeguards and homeland security and mapping its distribution have become high-priority tasks. To support these needs, Radiation Monitoring Devices Inc. has been actively researching and advancing the development of a coded-aperture gamma-radiation imager, RadCam™ [1-3]. This device has the capability of determining the radiation distribution, intensity, and energy from a distance. This is done by creating a radiation plot, via a nuclear camera, and overlaying the information upon a video image of the area being examined.

Recently, we have developed a data manipulation and storage scheme called the “data cube.” The data-cube technique allows a multi-dimensional array of data comprised of the x- and y-position coordinates, and the event energy, to be used in the imaging process. Gating along the different axes of the cube allows sophisticated analysis and visualization of radiation maps created by the imager, including the construction of 3-D images using a stereoscopic approach.

a. Radiation Imager Background

Radiation imagers for gamma radiation, in the range of 10 keV to 2 MeV use dense, high-Z apertures to modulate the radiation field. The aperture can be a single pinhole, or a pattern of small apertures arranged according to a mathematical encoding scheme. The aperture projects an encoded

image onto a position-sensitive detector coupled to a suitable scintillator. The position-sensitive detector is read out and the data are displayed via a data readout/storage scheme.

We have carried out extensive research and development optimizing the properties of radiation imagers to produce a spectroscopic, gamma ray imaging system, RadCam™. This system has high performance, excellent resolution, application flexibility, and is transportable. Figure 1 a) shows a photograph of the RadCam™ instrument, next to a table, b), describing the performance characteristics of the system.

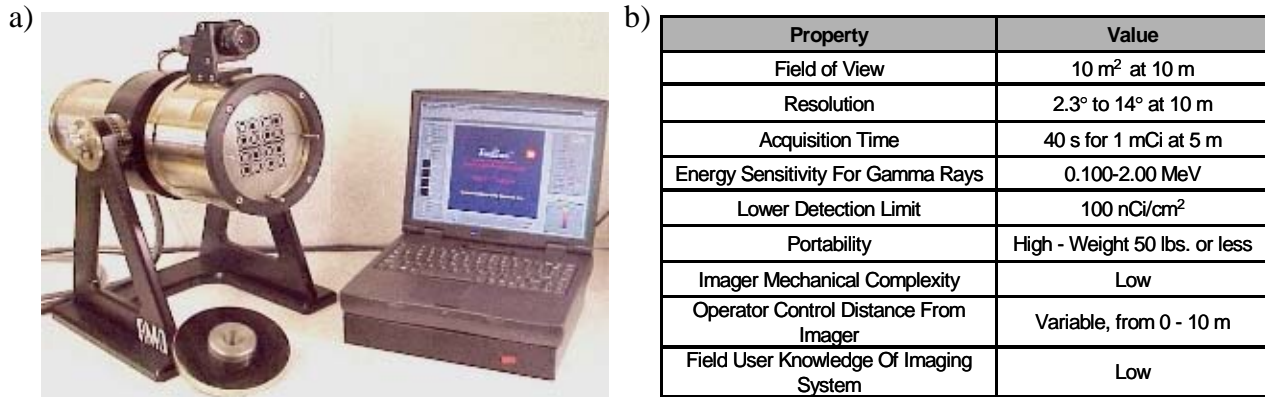


Figure 1. a) The RadCam™ is a dual-aperture, gamma-radiation imager with spectroscopic capability. b) The table lists the characteristics for the RadCam™ imaging system.

The primary components of the RadCam™ imager are a position sensitive photomultiplier tube, PSPMT (Hamamatsu R2486), a CsI(Na) scintillation crystal, and a tungsten, modified-uniformly-redundant-array (MURA), coded-aperture mask. The thin, 5 cm x 5 cm CsI(Na) scintillation crystal is optically coupled the face of the PSPMT. The axially centered PSPMT-scintillation detector is placed 6 cm behind the MURA aperture, and it generates 4 output signals from a position-sensitive, x-y-grid anode. These signals can be used to determine two key properties about the interaction of gamma rays with the scintillation crystal: energy and position. Summing the signal from the four contacts of the PSPMT produces the energy of the event, while partitioning the four contacts into various pairs, e.g., (1+2) and (3+4) for the y-position, and (1+4) and (3+2) for the x-position, produces the position coordinate for the location of the event in the scintillation crystal.

b. Coded-aperture and pin-hole imaging

The “shadow-gram”, or raw coded-aperture image, represents a superposition of the multiple “pinhole images” produced by each open hole in the coded-aperture mask, as illustrated in Figure 2 a). In essence, the mask encodes the image of the object by overlapping the individual pinhole images. The mask defines the encoding and, as described below, its mathematical representation is used to reconstruct the image of the object from the “shadow-gram” [1-6].

The MURA pattern has several important characteristics that optimize its performance as a coded-aperture mask. First, the modulation transfer function (MTF) of the MURA, which describes the transmission of the mask as a function of the object’s spatial frequency components, is relatively uniform. Second, the 50% open area of the mask maximizes the transmission of the incident radiation while providing an optimal MTF. Third, the inverse of the MURA pattern can be obtained by simply rotating the mask 90°.

The RadCam™ imager supports various imaging modes, and aperture masks, including the use of a single pinhole mask, a single coded-aperture mask, and a double coded-aperture mode, where the mask is rotated 90° to acquire the inverse of the single coded aperture image. Figure 2 b) and c) shows a comparison of the Gamma-ray images using these three different imaging modes, or configurations. Figure 2 b) shows the images produced by a single point source, for the pinhole, single coded aperture, and double coded aperture configurations. Figure 2 c) shows the images produced by a pair of point sources for these configurations, where one of the sources is located outside of the field of view (FOV).

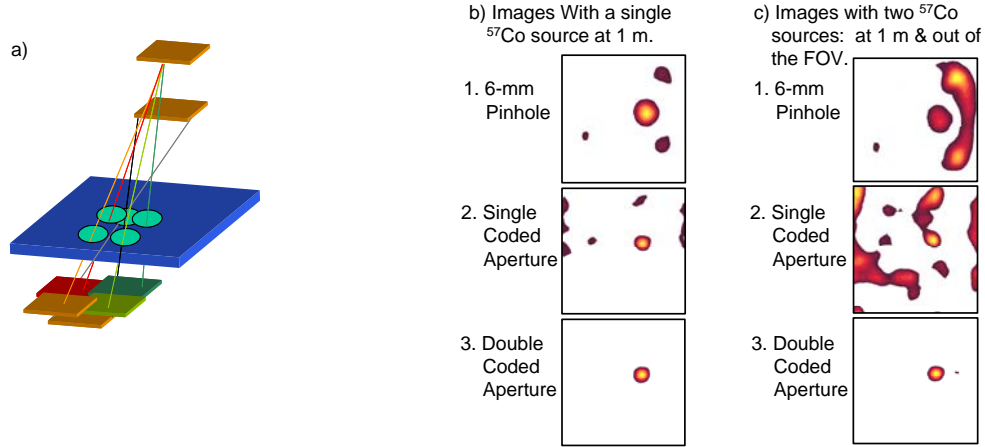


Figure 2. a) The illustration shows the overlap pinhole images produced by the coded-aperture mask. b) and c) Comparison of images acquired with the following apertures: 1. pin-hole aperture, 2. single coded aperture, and 3. double coded aperture. b) Images with a single ⁵⁷Co source at 1-m distance from the imager. c) Images with two ⁵⁷Co sources: one at a 1-m distance from the imager, and the other in a position that is out of the field of view (FOV).

As seen in Figure 2 b) and c), the double-coded aperture imaging mode produces superior images and the use of the inverse pattern eliminates background signal. For all the measurements described below, the RadCam™ imager was operated using the double-coded aperture mode of imaging, which is also referred to as the image/anti-image procedure. The controlling software of RadCam™ easily accommodates the different in image acquisition modes through a user selectable “Aperture Select” mode. The interchangeability of the apertures is quick and simple.

c. Image Reconstruction and the Data Cube

The "shadow-gram" produced by the coded-aperture is sampled by the PSPMT, held by a PSPMT I/O card, and then stored digitally via the analog capture card as the mask intensity array, $M(i,j)$. The image is then corrected for PSPMT non-linearity and gain variations across the tube face by reference to a look-up table. For a discretely-sampled, two-dimensional image, such as that generated by the RadCam™, the mask decoding pattern $D(i,j)$ can be correlated with the corrected mask-intensity array $M_c(i,j)$ to yield the reconstructed image data $R(k,l)$ as seen in Equation (1) [4-6].

$$R(k,l) = \sum_{i=1}^r \sum_{j=1}^r M_c(i,j) D[\text{mod}_r(i+k), \text{mod}_r(j+l)], \quad (1)$$

Here r is the number of apertures in the basic coded-mask MURA pattern along an edge and mod is the modulus operator. It was found, however, that the looping structure to determine $R(k,l)$ was computationally lengthy and a faster method was chosen. Since the calculations from Equation (1)

go as the number of terms squared, fast Fourier transforms (FFT) were used to reduce the calculations to the order of number of terms times the log of the number of terms. This resulted in a 35-fold improvement in processing speed and image generation. Equation (1) can be expressed as a convolution, shown in Equation (2), as well as the computationally more efficient FFT form, also shown in Equation (2).

$$R = M_c \otimes D = \text{FFT}^{-1} [(\text{FFT} (M_c) \times \text{FFT}(D))]. \quad (2)$$

Here \otimes is the correlation operator. The R data are displayed as the radiation image overlaid on a co-registered video image to make the radiation map.

In the past, the mask intensity array, $M_C(i,j)$, has been restricted to two dimensions, representing the x- and y-coordinates. We have developed a new mask intensity array, $M_C(i,j,E_n)$ that has an added energy dependence to produce a 3-dimensional data array of depth n . The FFT of each intensity level of energy bin n allows the creation of the subsequent mathematical entity $R(i,j,E_n)$, which we call the “data cube.” The data cube is an image, $R(i,j)$, for each energy level or energy bin. Through the IMAGE software of RadCam™ it is possible gate along any axis of the $R(i,j,E_n)$ array and, depending on the axis, extracts and energy-gated image, or a position-gated energy spectrum.

II. RESEARCH

RadCam™ images the position and distribution of suspected radiation sources. To do this, the imaging spectrometer is placed near a probable source, and the image is generated through the controlling software. After a user-selected time, or count, interval, the coded-aperture mask is rotated, producing the inverse mask pattern, and another image is taken. The final radiation image is generated and displayed on the laptop computer. The pseudo-color radiation image is overlaid on a co-registered video image of the same area captured by a high-resolution charge-coupled device (CCD). The combined (radiation plus video) image is then finally displayed as an accurate map of gamma-radiation sources in the physical environment. A Microsoft Windows™ 95/98/ME/2000/NT program, IMAGE 2000, which was developed for the imager, controls data acquisition and image display.

To demonstrate the effect of the data cube on radiation imaging, a series of images are given in Figure 3. There are three suitcases in the image. The leftmost suitcase contains a 100- μCi ^{22}Na source (511- and 1274-keV gamma rays), and the rightmost suitcase contains a 100- μCi ^{241}Am source (25- and 60-keV gamma rays). The third suitcase, in the middle of the image in Figure 3, is empty.

The image and graph to the left of Figure 3 are the data acquired during a RadCam™ data acquisition run. The image was acquired for an aggregate total of one million counts using a coded aperture image/anti-image procedure [1]. Two radiation sources, labeled in a purple-to-yellow intensity-color scheme, are clearly discernable when a 30% threshold is used to reduce background image contributions.

If a gate in the energy spectrum of the data cube is applied, images can be produced corresponding to that energy region. This is shown in Figure 3 c), where an energy gate around the ^{241}Am gamma-ray peak yields the ^{241}Am radiation image, the top image, and a gate around the ^{22}Na photo-peak

yields the ^{22}Na radiation image, the bottom image. The energy-gated images enable the identification and location of the different sources in the suitcases.

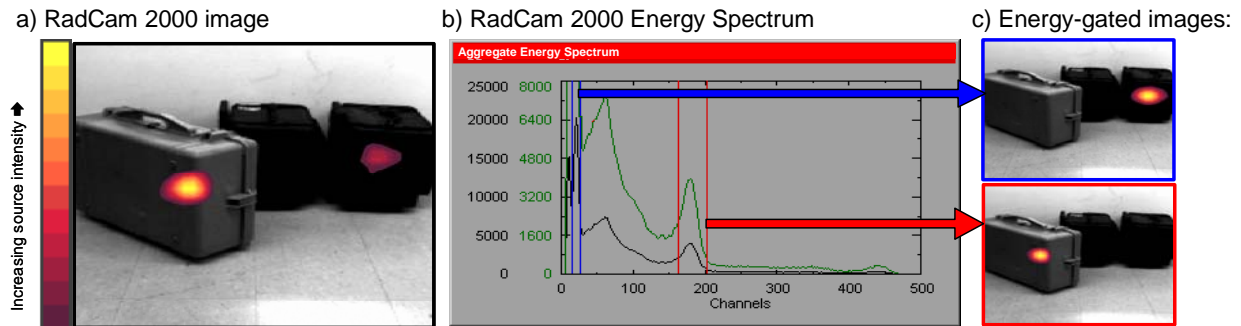


Figure 3. a) The visual image produced by RadCam™. In this measurement, a 100- μCi ^{241}Am source is in the right (black) case and a 100- μCi ^{22}Na source is in the gray suitcase to the left. The main image was acquired, in a count-based mode, for one million counts using a coded-aperture, image/anti-image technique. b) The graph shows the energy spectrum of the imaged sources. c) The images produced when a gate is applied to different regions of the energy spectrum. The energy-gated images enable the identification and location of the different sources in the suitcases.

If a gate in the energy spectrum of the data cube is applied, images can be produced corresponding to that energy region. This is shown in Figure 3 c), where an energy gate around the ^{241}Am gamma-ray peak yields the ^{241}Am radiation image, the top image, and a gate around the ^{22}Na photo-peak yields the ^{22}Na radiation image, the bottom image. The energy-gated images enable the identification and location of the different sources in the suitcases.

An example of the effectiveness of the gating and noise reduction procedures possible with the data cube, are demonstrated in an additional radiation image made using the imager. A 5-minute image of a 20-mCi ^{57}Co source (122-keV gamma rays) is shown in Figure 4.

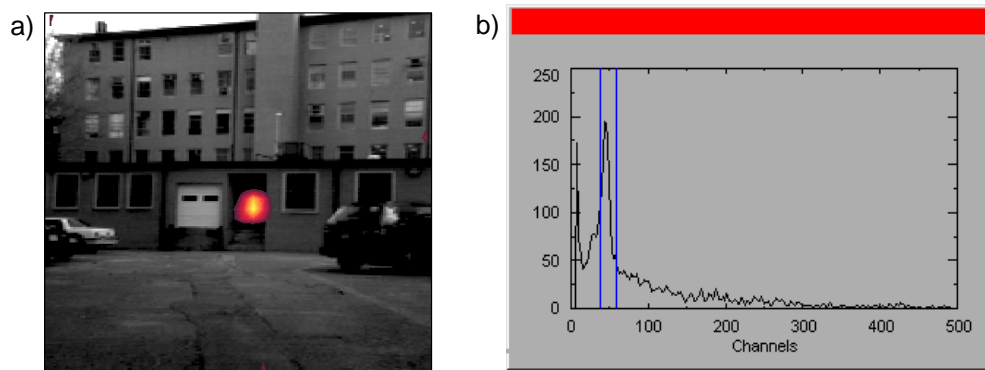
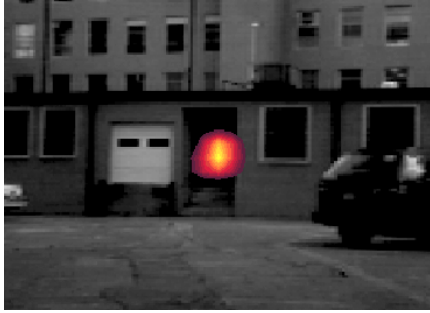


Figure 4. A RadCam™ image of a 20-mCi ^{57}Co source (122-keV gamma rays) on a lab bench of interior room. The image, a), was acquired 5 minutes when the distance between the source and imager was 70 meters. The blue lines in the energy spectrum centered around the 122-keV gamma-ray line in the ^{57}Co spectrum produce the image above.

The radiation source in this image is placed inside the building on a lab bench of an interior room approximately 70 m from the imager. As demonstrated by the image, the source is easily located within the imager field of view in the energy-gated image.

Figure 5, below, illustrates an operation where two RadCam™ images are used to stereoscopically locate the source in three dimensions (3-D).

a) RadCam200 Image



b) Proposed location in 3-D from stereoscopic approach

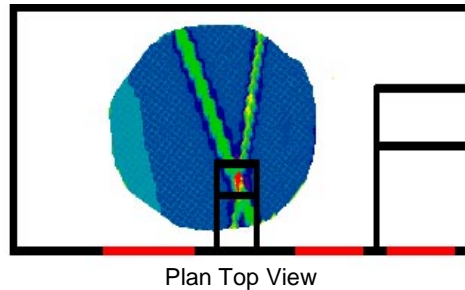


Figure 5. a) A RadCam™ image of a 20-mCi ⁵⁷Co source (122-keV gamma rays) on a lab bench of interior room. b) This illustration shows the proposed location, in 3-D, from a stereoscopic measurement.

The location of the source in a single image provides a line where the source is located. The second image extracts the actual distance, or position along the line, where the source is located, thus producing a 3-D rendering of the source location. In principle, it may be possible to extract the distance of the source from the imager using a single™ image.

Robotically deployed RadCam™

The basic radiation imager design was adapted for robotic deployment. The new system was much lighter and compact making it amenable for robotic deployment while still retaining the high performance of the original (RadCam™) imager. Figure 6, below, show a photograph of the robotically deployed camera, and an image that locates the radioactive material placed in the top canister.

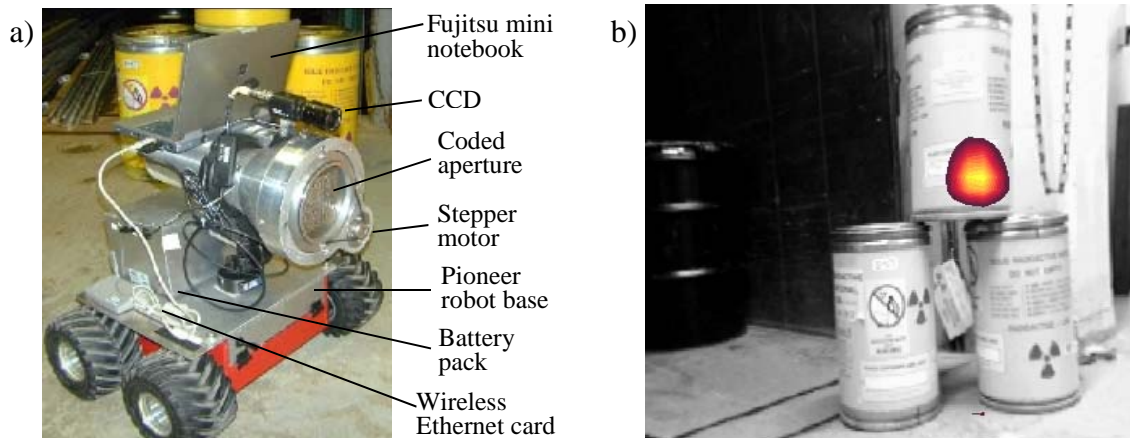


Figure 6. a) The photograph shows the assembled prototype robotic imager at the University of Michigan test site. The scale of the device is defined by the size of the robot tires, which are 4" in diameter. b) Image of a radioactive source located with the prototype robotic imager.

The performance of the robot-mounted, imager device was excellent, with similar performance to that of the RMD commercial, transportable version. The unshielded imager could create images in areas with radiation background over 30 times larger than the field-of-view source strength. The spectroscopic capability is a valuable feature for reducing background contributions and isolating single sources in a mixed field. The successful demonstration of wireless, robot-based mobility of the imager shows that the device can be moved into uncharacterized areas, without human exposure, and meaningful information can be recorded in a reasonable time.

IV. SUMMARY

The multi-dimensional gating techniques are very powerful for extracting information from radiation images generated by the RadCam™ imager. In fact, in most cases the energy-gating technique enables the location of sources that would otherwise go undetected. Position gating techniques are excellent for determining the distribution of specific types of isotopes in a given image. Future work will focus on extracting the location of the source in the third-dimension, which is the distance from the imager. The robot imager device based upon the PSPMT showed great promise and excellent performance characteristics in a robotically deployed application. This device is fully suitable for further development under more advanced research.

V. REFERENCES

- [1] M. Woodring, D. Souza, S. Tipnis, P. Waer, M.R. Squillante, G. Entine, K.P. Ziock, "Advanced Radiation Imaging of Low-intensity Gamma-ray Sources," NIM in Physics Research A, 422, pp. 709-712, 1999.
- [2] M. Woodring, D. Souza, F. Thatch, M.R. Squillante, G. Entine, D. Wehe, Proc. 42nd INMM Annual Meeting, Indian Wells, CA, July 15-19, 2001. *A Robotically Deployed, Spectroscopic, Gamma-ray Imager.*
- [3] M. Woodring, D. Souza, L. Honig, M. Squillante, G. Entine, Proc. SPIE 44th Conference Optical Science, Engineering, and Instrumentation, Denver, CO., 18-23 July, 1999, Penetrating Radiation Systems and Applications, F. Patrick Doty, Ed., 3769 (1999) 234-242.
- [4] E.E. Fennimore, T.M. Cannon, "Coded Aperture Imaging with Uniformly Redundant Arrays," Applied Optics, 17, No. 3, pp. 337-347, 1978.
- [5] S.R. Gottesman, E.E. Fenimore, "New Family of Binary Arrays for Coded Aperture Imaging," Applied Optics, 28, No. 20, pp. 4344-4352, 1989.
- [6] E.E. Fennimore, T.M. Cannon, "Uniformly Redundant Arrays: Digital Reconstruction Methods," Applied Optics, 20, No. 10, pp. 1858-1864, 1981.

VI. ACKNOWLEDGEMENTS

The authors would like to thank David Beddingfield and David Wehe for their valued contributions during the course of the RadCam development project. The authors would also like to thank Dr. Johann Borenstein, Engineer James Berry, and Christopher W. Becker, and his staff, for assisting with the robotically deployed RadCam™ measurements. This work was carried out with partial support from DOE (Contract #DE-FG02-00ER83087).